Journal of Applied Fluid Mechanics, Vol. 17, No. 4, pp. 785-798, 2024.
Available online at www.jafmonline.net, ISSN 1735-3572, EISSN 1735-3645.
https://doi.org/10.47176/jafm.17.4.2200

Effect of Blade Slot Positioning Close to Blade Root on the Performance of Highly Loaded Helium Compressor

Y. Fan[1], Z. Tian[1†], A. Malik[2], P. Ren[1] and J. Zheng[1]

[1] *Naval Architecture and Ocean Engineering College, Dalian Maritime University, Dalian, Liaoning Province, 116026, China*
[2] *Pakistan Navy Engineering College, National University of Sciences and Technology, Islamabad, 44000, Pakistan*

†Corresponding Author Email: tianzhitao@dlmu.edu.cn

ABSTRACT

The helium compressor has the inherent characteristics of a lower single-stage pressure ratio and a higher number of stages than an air compressor. The highly loaded design method effectively addressed the compressibility issue of the helium compressor. However, the compressor designed with this technique has narrow passages, short blades, and a large bending angle, making the end-wall secondary flow more intense than a conventional compressor. In this paper, numerical simulation and experimental validation has been conducted to identify the effectiveness of the axial slot close to the blade root in improving end-wall secondary flow in a high-load helium compressor cascade, and to provide data and experimental support for the engineering application of high-load helium compressors. The analytical results show that slotting can utilize the self-pressure difference to generate gap leakage vortices, and the axial momentum generated by the leakage vortices blows away the vortices formed due to the separation of corner area. The airflow flows close to the suction surface of the blade and breaks away at the trailing edge of the blade, merges with the main flow and forms a new vortex. As the height of the channel increases, the blowing away of the vortices in the corner region becomes more pronounced and the cascade improvement performance is better. The test results show that the total pressure loss coefficient at the design operating point is reduced by 6.167% when a slot height of 8.53 mm is positioned at 65% Ca (axial chord length). The improvement effect becomes 16.469% better at a 4° attack angle.

Article History

Received July 29, 2023
Revised November 11, 2023
Accepted November 24, 2023
Available online January 30, 2024

Keywords:

Helium compressor
Blade root slotting
Total pressure loss
Highly loaded design
Improvement coefficient

1. INTRODUCTION

Nuclear energy has the inherent benefit of reducing carbon emissions and its good stability and high efficiency throughout its life cycle (Ye et al., 2022). The future development trend of nuclear energy is toward the fourth generation of nuclear energy systems. HTGR is one of the typical types of fourth-generation nuclear energy systems because of their better safety, higher power generation efficiency, and broad application range (Kadak, 2016). Helium is one of the best coolants in HTGR that removes heat from the reactor core. It is considered an ideal inert gas because of its stable chemical properties, negligible effect on neutrons in the reactor at high temperatures, and good thermodynamic performance. Helium, as the working medium, is compressed in a helium compressor, whose performance directly affects the power output of the system(Tian, 2019). However, helium has a high specific heat ratio, which makes it difficult to compress (El-Genk & Tournier, 2008). Therefore, modern helium compressors have lower single-stage pressure ratios and a higher number of stages, which leads to issues in increasing the power density and consequently affects the commercialisation of HTGR. For example, the Oberhausen II 50 MW helium turbine has 25 high- and low-pressure compressor stages with a pressure ratio of just 2.7 (Weisbrodt, 1996).

Scholars at home and abroad have conducted several studies to address the aerodynamic performance issues with helium compressors. (Malik & Zheng, 2020) mixed helium with xenon and discussed the influence of mixed coolant on compressor performance in power conversion units of HTGR. Mixing helium and xenon raised the pressure ratio while maintaining good heat transfer because xenon could be easily compressed. The 15g/mol helium-xenon mixture produces a high heat transfer coefficient of 7% and a higher outlet pressure. (Chen et al., 2019) developed a similar method that can be used to

NOMENCLATURE

β_1	geometric intake angle	ξ	relative blockage coefficient
β_2	geometric outlet angle	π	static pressure ratio
C	chord length	t	pitch length
H	cascade height	Ca	relative chord length position
κ	turbulent kinetic energy	ω	turbulent dissipation rate
z/Z	relative axial chord length	h/H	relative blade height
P	static pressure at measuring point	P^*	total local pressure
P_{in}	static pressure at the inlet	P^*_{in}	total pressure at the inlet
Q_m	slotted outlet flow rate	P^*_{out}	total pressure at the outlet
$v_z(x,y)$	flow velocity	ρ_{fs}	mainstream density
V_{fs}	mainstream velocity	i	attack angle
Cp_t	total pressure loss coefficient	Cp	static pressure coefficient
Cp_{to}	total pressure loss coefficient of prototype cascade	Cp_{ts}	total pressure loss coefficient of slotted cascade
$\Delta Cp_{t\%}$	improvement coefficient	*HTGR*	High Temperature Gas-Cooled Reactor

obtain the performance characteristics of helium compressor through experiments on air compressor. Hence, saving the experimental cost of the helium compressor. Ke and Zheng (2010, 2011) verified the use of the highly loaded design method through numerical calculation and successfully increased the single-stage pressure ratio of the helium compressor from 1.03 to 1.08 (Ke & Zheng, 2012). Similarly, (Tian, 2019) took the 16-stage low-pressure helium compressor used in the 300MW HTGR developed by the Japan Atomic Energy Research Institute as the prototype and optimized its design scheme by reselecting the parameters. Accordingly, the compressor stages were reduced to 4 with similar aerodynamic performance. The compressor with a highly loaded design technique has short blades, more considerable blade curvature, and a higher reverse pressure gradient. Consequently, the boundary layer part increases with the intensive secondary flow at the end wall (Tian et al., 2019).

Blade slotting is a traditional passive control method that reduces or blows away the separation of three-dimensional corner area. This method is suitable for the helium compressor of a closed Brayton cycle because it does not require external energy. (Brent, 1972) first proposed the slotted-blade design technique in 1972. They used the NACA-65 series as the test blade and designed a three-tooth slot structure on the rotors and stators. Blade slotting increased the diffusion factor of the rotor tip from 0.53 to 0.7 and that of the stator hub from 0.6 to 0.76. Ramzi et al., 2011) discussed the potential of the passive control of slotted blades under stall conditions. Accordingly, numerous numerical studies have demonstrated that the loss can be decreased by 28%, and the flow turning angle can be increased by up to 5° in two-dimensional cases. In the three-dimensional flow field, the advantage of the groove is more prominent, which can delay the boundary layer separation after 50% of the chord length. Yoon et al. (2019) used a high-speed compressor (HSRC) as the research object and conducted a numerical analysis using a flow control method. It was observed that a slot close to the end wall with a span of less than 10% could improve the stall margin by 6%. Through the slot, the separation near the hub weakened and eliminated the source of corner separation. Liu (2016) investigated the possibility of controlling the divided flow by slotting the blade root. The results showed that root slotting could reduce the corner separation of the cascade and improve the flow conditions on the suction surface. Zhao et al. (2021) used different clearance schemes to study the influence of slotting on compressor stability. It was concluded that partial clearance of the stator blades could broaden the compressor stall margin under low operating conditions. The leakage flow generated by the clearance significantly eliminates the stall vortex in the corner, consequently improving the compressor stall margin.

This study analyzed the influence of blade slots on a highly loaded helium compressor. The research object was a high-load blade profile designed based on the thermophysical properties. The control effect of the shape and height of the slot close to the blade root on the corner separation of the stator blade was investigated using a numerical simulation with helium as the working fluid. Finally, the optimal slotting arrangement was determined and experimentally verified to improve the performance of the helium compressor cascade. This study provides a reference for the slotting effect on the blade root of a helium compressor.

2. NUMERICAL AND EXPERIMENTAL METHOD

2.1 Numerical Method

2.1.1 Physical Model

The reference cascade analysed in this study is the fourth-stage stator of a high-loaded helium compressor at 50% blade height. The cascade exhibits a large bending angle, high loading, and low aspect ratio. The cascade parameters are shown in Fig.1.

2.1.2 Grid and Calculation Method

The computational blade channel grid used in this study was generated using Numeca-AutoGrid5. It adopts the HOH topology. The slotted portion was generated using the Numeca-IGG module, and the shape of the channel was determined by changing the positions of the nodes in the channel. To ensure calculation accuracy, the number of grid nodes at the lead and trail edges of the

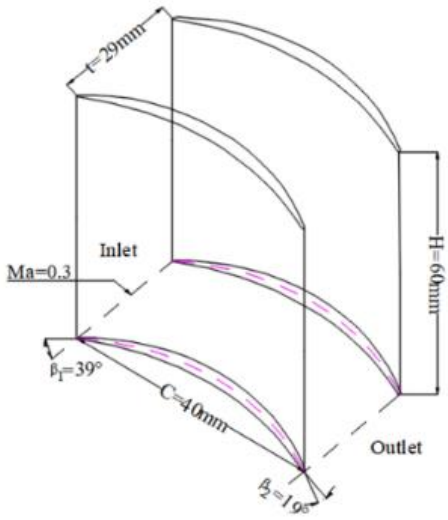

Fig. 1 Definition of aerodynamic and geometric parameters of cascade

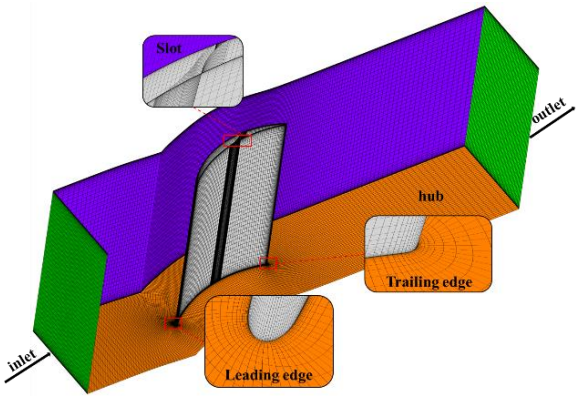

Fig. 2 Diagram of cascade and slotted grid

blade, upper and lower end walls, blade surface, and slot boundary were increased. The grid structure is illustrated in Fig.2.

The numerical research was conducted using the CFX module of the commercial software ANSYS. The axial chord length from the leading edge of the cascade to the inlet of the computational domain was 1.5 times, and that to the outlet was 2 times. Helium gas was used as the working medium. The total temperature at the inlet was 300K, and the turbulence intensity of the fluid was 5%. The inlet Mach number was kept at 0.3 by adjusting the total pressure, and an average distributed static pressure was set at the outlet. Translational periodicity interfaces are set on both sides of the flow passage.

The grid independence of the prototype cascade grid and the grid of the slotted structure were validated to reduce calculation costs and ensure accuracy. The outlet section was selected for data processing. As the total pressure loss coefficient accurately represents the flow situation in the cascade flow passage and the cascade's overall performance, the total pressure loss coefficient at the outlet section of the cascade was selected as the reference parameter. The total pressure loss coefficient is defined as follows:

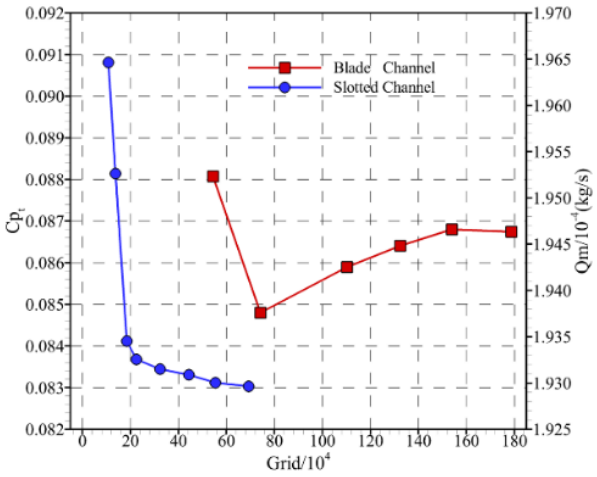

Fig. 3 Verification of grid independence of cascade and slotted channel

$$Cp_t = (P_{in}^* - P_{out}^*)/(P_{in}^* - P_{in}) \quad (1)$$

As illustrated in Fig.3, cascade grids increased from 0.5 million to 1.8 million in six steps. At a grid size of 1.54 million, the total pressure loss coefficient variance was relatively minimal. Therefore, a 1.54 million grid size is selected as the grid size of the prototype cascade, considering calculation costs. For the blade slotting, the mass flow rate at the outlet of the slotted channel was selected as the reference parameter. The grid size in the slotted areas increased from 0.1 million to 0.7 million in eight steps. It can be seen from the curve that the outlet flow of the slotted channel decreases with the increase in the grid size. The outlet flow stabilised when the grid size exceeded 0.22 million. Therefore, a 0.22 million grid size is selected for the slotted region. Accordingly, the slotted channel grid nodes increased to different degrees with the change in the slotted channel height.

2.2 Experiment introduction

2.2.1 Experimental Equipment

Helium wind tunnel tests require costly seals and sufficient helium. It has been shown in the literature (Tian et al., 2021) that an air-working fluid with equal inlet Mach and Reynolds numbers and lower Mach numbers can reflect, to some extent, the flow of the helium working fluid inside the cascade. Therefore, the experiments in this study used air instead of helium as the working fluid and the feasibility of using air instead of helium as the working fluid was verified. The cascade was tested on a subsonic cascade wind tunnel test bench at the Dalian Maritime University. The major components of the test bench and cascade are shown in Fig.4. The wind tunnel was a continuous normal-temperature open-jet wind tunnel. The requisite airflow was achieved using a centrifugal fan, and the inlet Mach number was regulated by adjusting its speed. The working fluid successfully enters the pressure diffuser section and the pressure stabilising and contraction sections. The effective exit of the test section was rectangular with dimensions of 255 × 60 mm. An electrical machinery control structure was installed on the

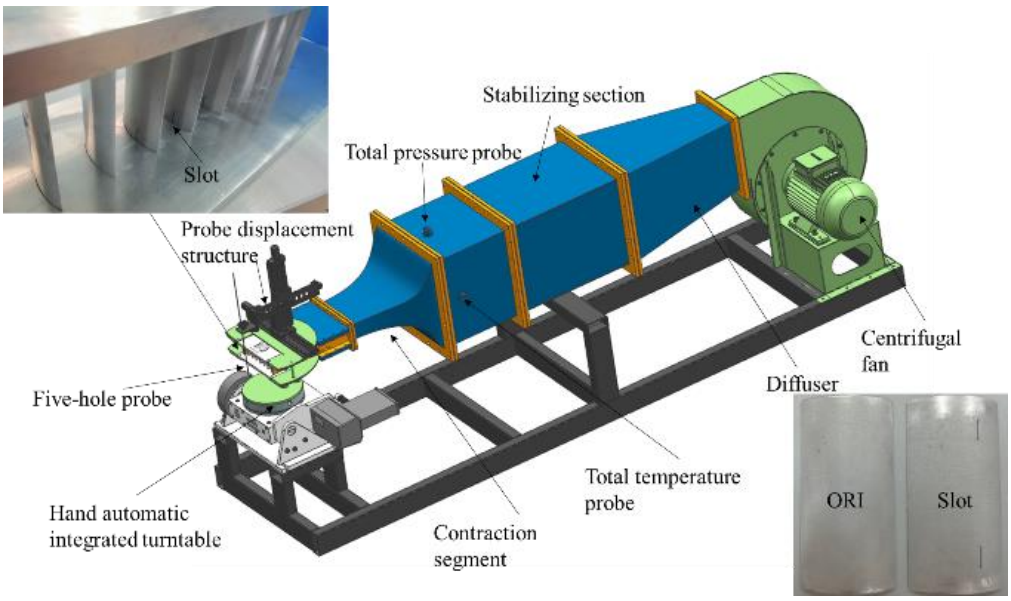

Fig. 4 Layout of the wind tunnel and test cascade

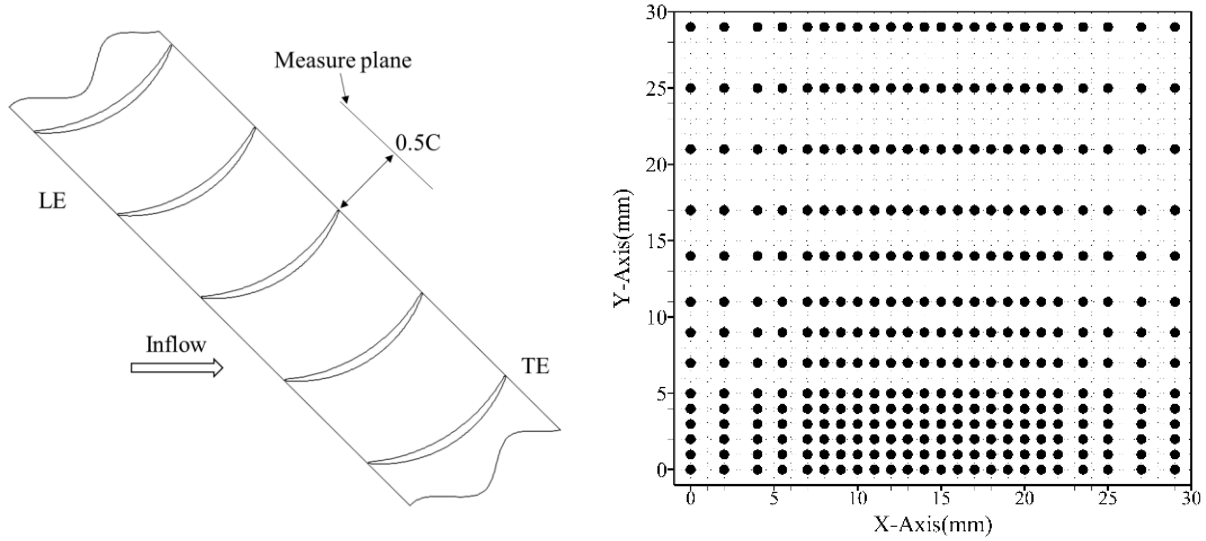

(a)Measurement plane (b)Measurement points

Fig. 5 Layout of measurement plane and measurement points

test bench to enable the movement of the five-hole probe on the two-dimensional plane. The turntable installed at the bottom of the test section can rotate clockwise and counterclockwise using a hand wheel or motor to achieve different incoming flow attack angles. Both the slotted and prototype blades were fabricated using 3D printing technology to guarantee the precision of the slotted profile and consistency of the surface roughness. The installation position was reserved in the height direction of the blade to allow the initial position of the slot to be directly attached to the end wall.

2.2.2 Experimental Method

The total inlet temperature and pressure were measured using a probe at the end of the pressure-stabilising section. Outlet airflow parameters were measured using a five-hole probe. The five-hole probe was located at the 50% chord-length plane from the blade's trailing edge and moved along the coordinated axis trajectory, as shown in Fig. 5(a). There were 336 test points distributed throughout 14 rows and 24 columns. A higher density of test points was observed in the wake and end wall areas, as shown in Fig.5(b).

The actual flow in a cascade channel can be simulated accurately using a suitable turbulence model. This paper selects three turbulence models (k-ε, k-ω, and SST), and numerical calculation was conducted with design attack angle and Mach number. Figure 6 shows the distribution of the total pressure loss coefficient at the outlet section for the three turbulence models and the experimental results. The loss contour obtained with the SST turbulence model was the closest to the experimental results. Therefore, the SST model was used in subsequent numerical simulations. A description of the theoretical basis of the SST turbulence model is available in the literature (Li et al., 2023), which describes turbulent kinetic energy κ, turbulent dissipation rate ω and turbulent eddy viscosity.

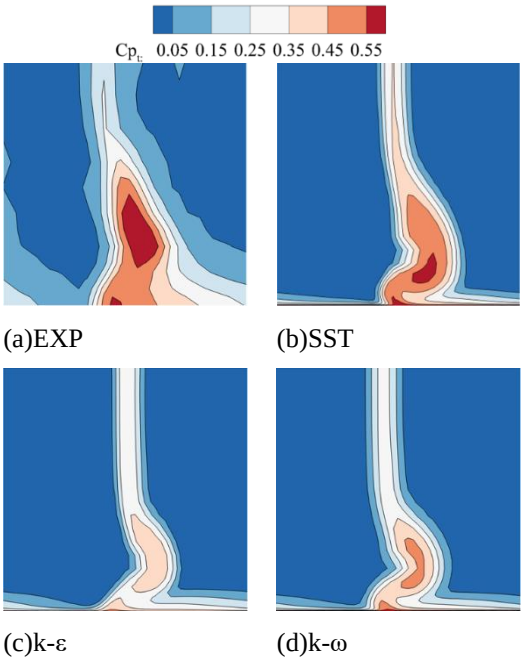

Fig. 6 Turbulence model verification

3. NUMERICAL RESULTS AND DISCUSSION

3.1 Influence of Slot Shape on the Performance of Cascade

3.1.1 Location Of Entrance Point of Slotted Channel

Previous research (Zhao at al., 2022) on blade slots has shown that a slot at the midsection of the blade might increase the compressor stall margin. However, it has a more detrimental effect on efficiency. The trailing-edge slot had the most negligible impact on the efficiency. However, it had the least ability to increase the stall margin. The rear slot is maintained between the middle and trailing edges of the blade. Meanwhile, the angle separation advanced when the attack angle of the incoming flow increased. Therefore, the upstream point of the slotted channel outlet, point B, was chosen as the benchmark and positioned at 65% of the axial chord length. Accordingly, points A, C, and D were chosen at suitable locations based on the benchmark points and the arrangement of the grid nodes. In this case, points A, C, and D were located near 50 %, 60%, and 68% Ca, respectively. The profile near the leading edge (AB) is more prone to separation owing to the Coanda effect, which significantly affects cascade performance. Therefore, based on the aforementioned technique, the position of point A is adjusted upstream, keeping the other points, that is, positions B, C, and D, unchanged. The geometry of the slotted channel is shown in Fig.7. The entrance areas of A_1 are the smallest, and A_4 are the broadest, respectively. In this section, full blade height slotting is adopted, and the effect of channel height on the cascade performance is not analysed.

The numerical calculation under the design conditions validated the positive effects of the axial slot position and slot arrangement. The total pressure loss coefficient results are shown in Fig.8. The improvement coefficient was defined as follows:

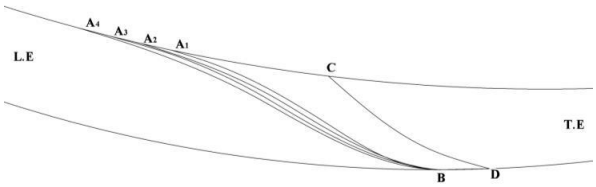

Fig.7 Display of slot axial position and slot control point

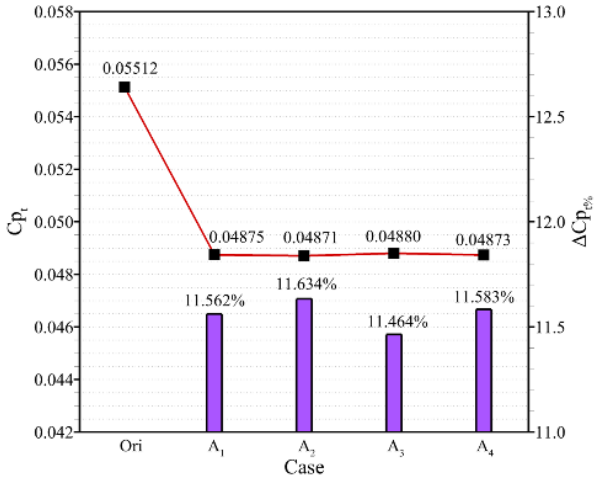

Fig. 8 Total pressure loss coefficient and improvement of different points A

$$\Delta Cp_{t\%} = (Cp_{to} - Cp_{ts}) / Cp_{to} \quad (2)$$

Here, Cp_{to} is the total pressure loss coefficient of the prototype cascade, and Cp_{ts} is the total pressure loss coefficient of the cascade with the addition of a slot. It can be seen that the four arrangements are effectively reduce the total pressure loss of the prototype cascade. The numerical calculation results are presented in Fig.8. The maximum optimisation effect was obtained once the upstream inlet was fixed at the A_2 position. At this time, the position of point A was near 48% Ca from the leading edge of the blade. In this arrangement, the total pressure loss coefficient was 0.04871, which was 11.634% better than that of the prototype cascade.

3.1.2 Slotted Channel Profile

In order to direct the fluid to a specific angle in the channel, both ends of the slotted channel profile should be tangential to the blade profile. In this section, the slotted profile is further improved based on the deductions from the previous section. Once the control points were set, five profile arrangements with reasonable variations in curvature were selected. These five arrangements were named Case 1 to Case 5, as shown in Fig. 9. The flow capacity at the outlet section of the slotted channel and the total pressure loss coefficient of the cascade are shown in Fig.10. It can be seen that the greater the flow rate in the channel, the smaller the cascade loss when the inlet and outlet areas are fixed. The profile design in Case5 increases the flow capacity of the slotted channel and minimises the cascade loss. The total pressure loss

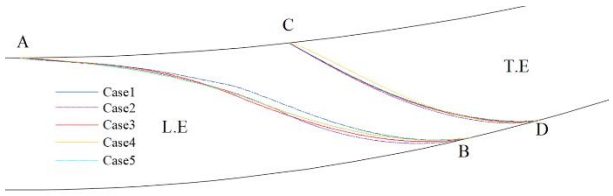

Fig. 9 Layout scheme of slotted profile

coefficient in Case 5 was 0.04846, and the improvement coefficient was 12.095%.

Figure 11 illustrates the total pressure loss contours for the five slotted profile schemes, where the high-loss area in Case 5 is the smallest. Case 1 and Case 3 have similar results. Case 2, Case 4, and Case 5 had similar results. As can be seen from the characteristics of the profiles displayed in Fig. 9, the Case 1 profile changes abruptly, resulting in a sudden reduction in the flow area of the channel. The second half of the Case 3 profile is nearly straight and may not adapt to the fluid flow in the slotted channel. After the calculation, it can be observed that profile AB is as tangential to the blade surface as possible at the entrance and exit. The transition in the middle section is reasonable, which can obviously improve the cascade. The change in the grooving profile significantly affected the loss area at the boundary layer, high-loss area close to the wall, the loss area near the middle of the blade, and the radial area of the loss area. The reasonable slotted profile increases the acceleration of fluid flow in the channel, so that the fluid at the outlet of the channel has enough momentum to suppress the backflow phenomenon at the corner of the stator, thus mutually inhibiting the vortex structure at the corner.

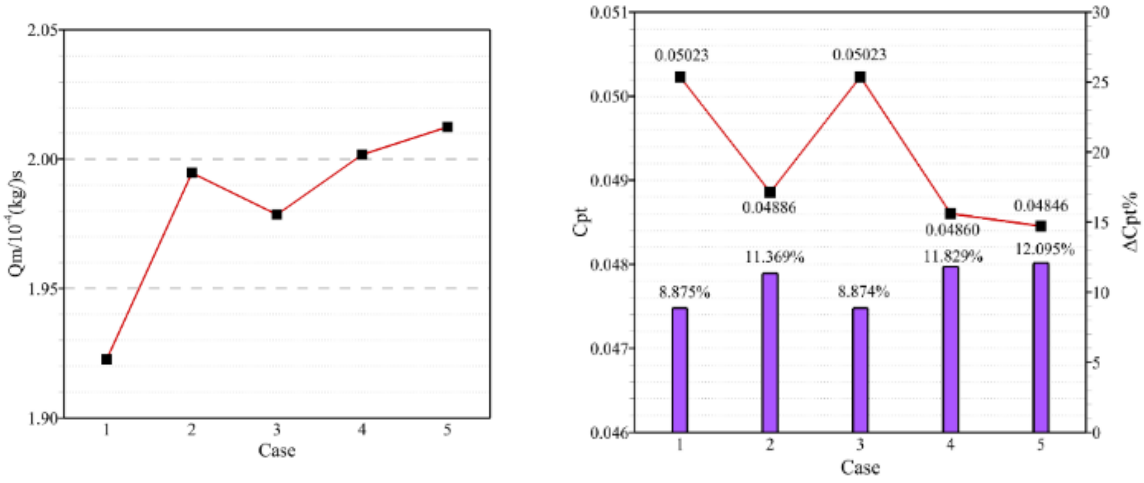

(a) Flow capacity of slotted channel outlet (b) Loss of different slotting profile arrangements

Fig. 10 Selection of slotting profile arrangement

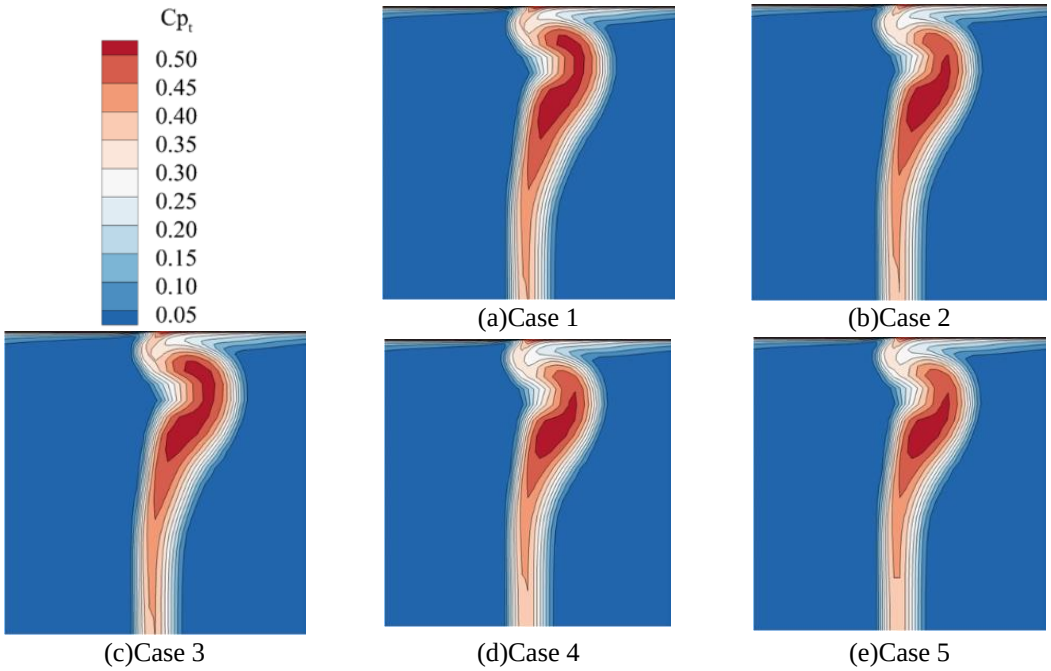

(a)Case 1 (b)Case 2

(c)Case 3 (d)Case 4 (e)Case 5

Fig. 11 Contour of total pressure loss at the outlet section

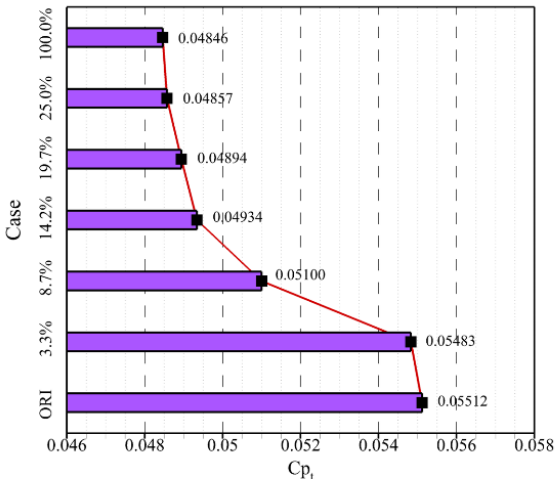

Fig. 12 Outlet cross-section losses for different slotted height arrangements

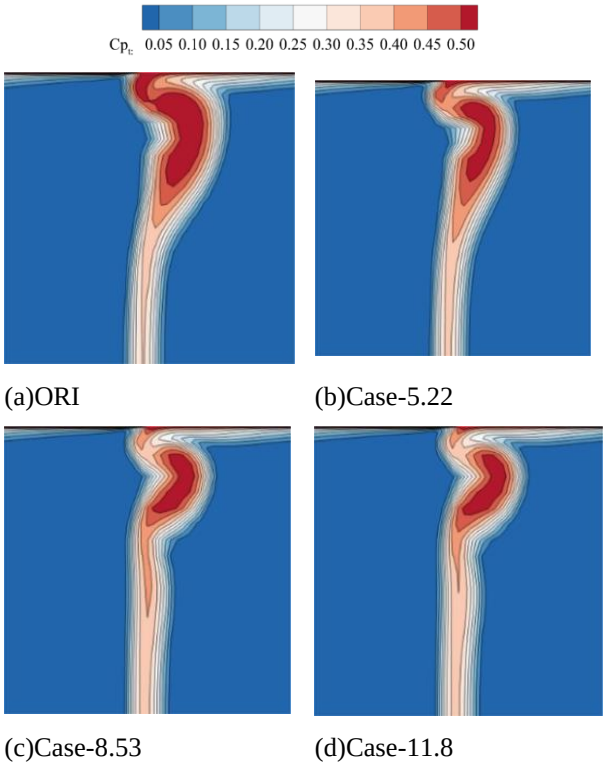

Fig. 13 Contour of total pressure loss at the outlet section

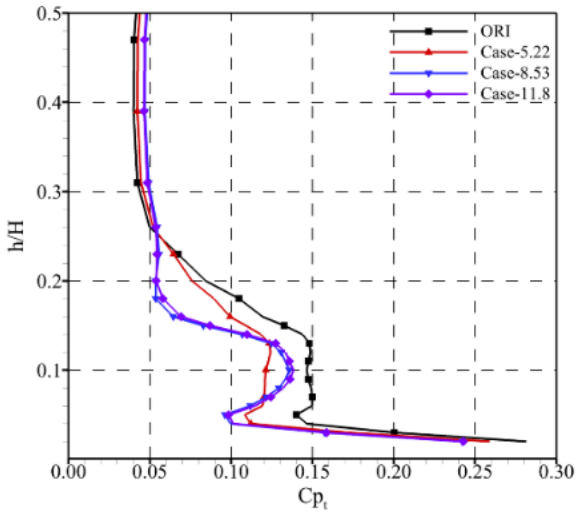

Fig. 14 Outlet cross-section losses along the blade height for different slotted heights

3.2 Influence of Slot Height on the Performance of Cascade

3.2.1 The Analysis Results of Design Angle of Attack

The full blade-height slotting technique is a challenging control method because it alters the blade geometry to minimise separation and enhance performance. Selecting an appropriate channel height can effectively control the separation flow while considering the structural performance of the blade. In this section, different slotting heights are analysed with the established slotting positions and profiles at the designed angles of attack. For the analysis, six different working conditions were designed based on the relative blade heights of 3.3%, 8.7%, 14.2%, 19.7%, 25%, and the full-blade height. The number of spanwise grid nodes increased with a change in the slot height. Fig. 12 shows the total pressure loss coefficient of the outlet cross-section for different arrangements.

The results in Fig. 12 show that the total pressure loss coefficient of the cascade does not change obviously with the further increase of the slot height. The total pressure loss coefficient change for full-blade-height slotting compared to 19.7%H slotting is only 1%. To explore the influence of the slot height on the cascade performance analysis, three different schemes were designed based on the relative blade heights: 8.7%, 14.2%, and 19.7%. Because the blade height was 60mm, the three schemes were named Case-5.22, Case-8.53, and Case-11.8, respectively. Figure 13 shows the total pressure loss contours in the prototype cascade and the cascade with three different slotted channel heights. The prototype cascade has a large-scale separation concentrated in the corner region, and the middle diameter loss is less than that in the other cases. Each slotting arrangement significantly inhibits the loss caused by the accumulation of low-energy flow clusters on the suction surface. The loss range is also reduced. Case-8.53 significantly changes the flow field behind the cascade, resulting in significant compression of the spanwise height of the loss region. Furthermore, Case-8.53 has a better impact on reducing the end wall boundary layer than Case-5.22. However, the loss zone close to the centre of the blade widened. As the slot height increased further, the light red wake loss under the high-loss area of Case-11.8 reduced, and the loss at the mid-diameter narrowed. No significant variation was observed in the blowing effect on the boundary layer or the core position of the high-loss area.

Figure 14 shows the distribution of the total pressure loss for different arrangements. By analysing and comparing the change in loss between the prototype cascade and the slotted cascade, it is possible to compare

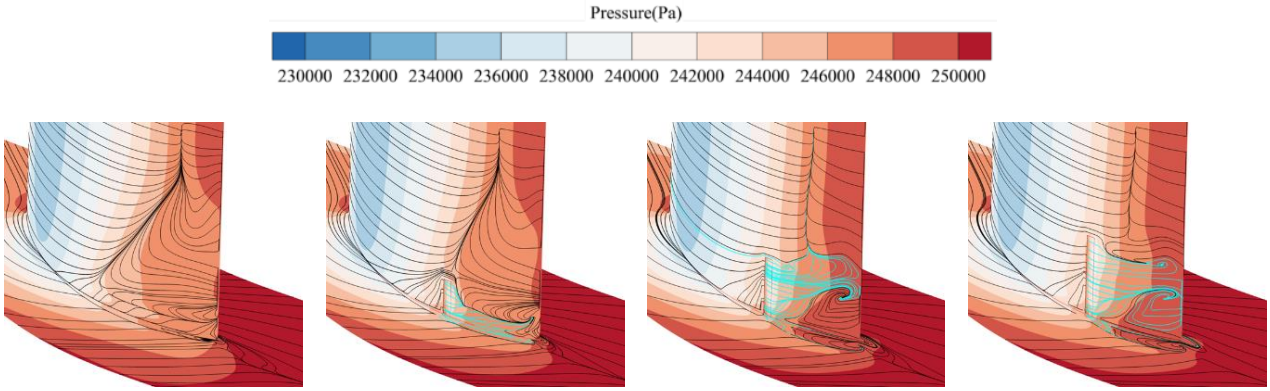

(a)ORI (b)Case-5.22 (c)Case-8.53 (d)Case-11.8

Fig. 15 Static pressure distribution and the limit streamline on the suction surface

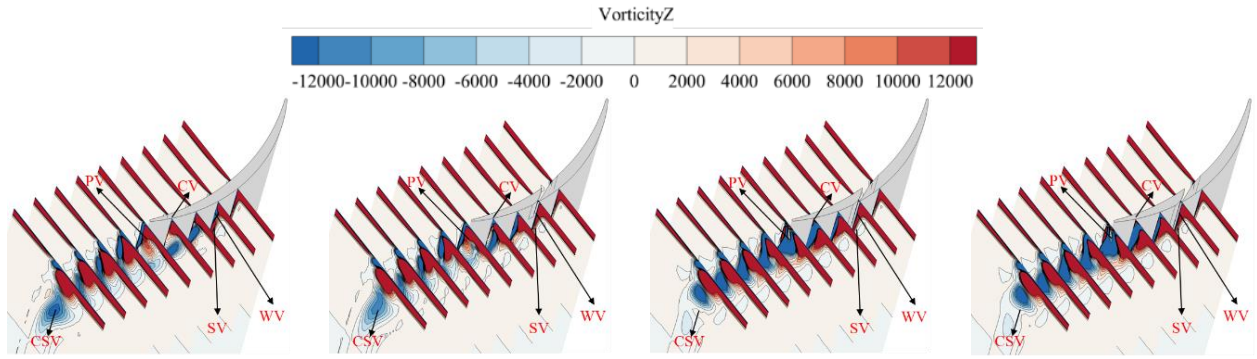

(a)ORI (b)Case-5.22 (c)Case-8.53 (d)Case-11.8

Fig. 16 Contour of axial vorticity of the S3 section

changes in the outlet span loss. The height loss ranged from the end wall to 25%H in the prototype cascade. The slotting arrangement at the root resulted in less than 25%H losses. In addition, the corner loss coefficient is reduced. However, a slight increase in loss from 25%H to the middle of the blade was observed. Case-8.53 gives a better blowing impact on the end-wall boundary layer within 6%H. In the range of 6–12%H, the circumferential width of the loss region broadened because the slot height increased. An increase in the slot height significantly reduced the loss in the range of 12%H~25%H. This confirms that an increase in height can further reduce the spanwise height of the loss. Meanwhile, it can be observed that the loss trajectories of Case-8.53 and Case-11.8 almost overlap. This phenomenon was consistent with the loss pattern shown in the contour of the total pressure loss.

Figure 15 shows the static pressure distribution contour and limiting streamline on the suction surface of the cascade. The flow capacity of the cascade was improved using a slotted channel arrangement with different heights. In Case-5.22, the flow at the end wall and suction surface were similar to those of the prototype cascade. Because the channel height of this arrangement was also low, the elevation height of the corner area was the same as that of the prototype cascade. Accordingly, the spanwise vortex structure at the trailing edge, generated by the interaction of the pressure surface backflow and the suction surface-end wall, disappeared. The influence of slotting on the flow field in the corner was significant in Case-8.53. In this case, the separation lines below the channel height disappeared. Part of the fluid flowing out of the slotted channel was elevated in the spanwise direction by the backflow of the boundary layer (near the trailing edge and end wall). Furthermore, there was a significant increase in static pressure at the trailing edge. Case-11.8 has a larger slot height, which allows for a broader range of influence of the fluid at the outlet of the channel but produces almost the same beneficial effect as Case-8.53, with a similar vortex structure in the trailing edge corner area and almost the same high hydrostatic pressure region contour for both schemes. The leakage flow generated by slotting has obvious jetting property. With the increase of slot height, two obvious vortex points appear on the hub surface. Among them, the small vortex point is the companion vortex induced by the leakage vortex jet, and the other vortex point is the radial vortex formed by the confluence of the jet and the main stream. Leakage flow on the suction surface inhibits the influence of some of the lower end-wall surface layer boundary on the main flow, and the helicity of the concentrated shedding vortex(CSV) is weakened.

Figure 16 shows the axial vortex contours of cross-section S3 for different slot height arrangements. The main effects of slotting are concentrated shedding vortex (CSV), passage vortex (PV), and wall vortex (WV). In Case-5.22, the vorticity of the CSV decreased compared with that of the prototype. Moreover, the vortex core began to move towards the blade root. Both the vorticity and influence range of the PV decrease and the circumferential range of the WV also decreases. The

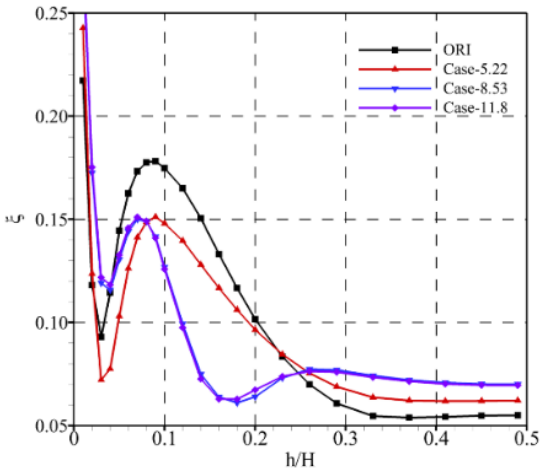

Fig. 17 Spanwise distribution of relative blockage coefficient of the outlet section

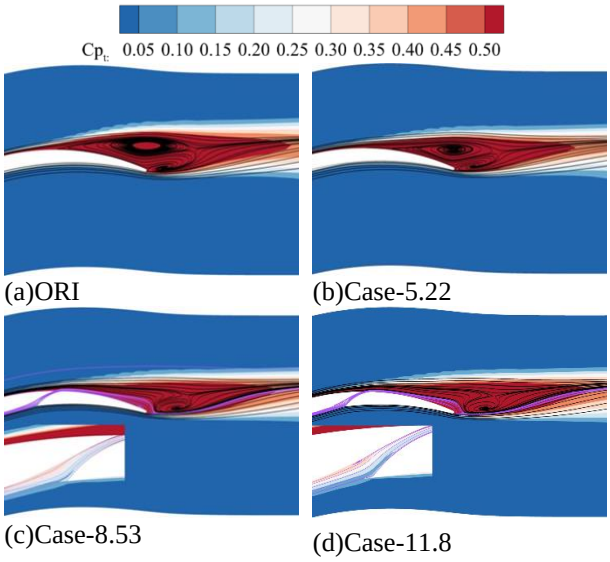

Fig. 18 Total pressure loss and streamline distribution in 10% blade height section

vortex structure behind the trailing edge changed significantly with increased slot height. The CSV increases in vorticity but decreases in the influence range under the action of slotting, and its influence on the fluid at the centre of the blade is weakened. The PV further reduces the CSV and leakage owing to slotting.

This study defined the relative blockage coefficient to quantitatively evaluate the improvement in the cascade flow capacity by slotting. This equation is formulated as follows:

$$\xi^*(x) = \int_0^{\xi} \{1-[\rho v_z(x,y)]/\rho_{fs}V_{fs}\}dy \tag{3}$$

$$\xi^*_{eff} = [\xi^*(x) - \xi^*_{mid}]/t \tag{4}$$

Figure 17 shows the distribution of the relative blockage coefficient of the outlet section in the spanwise direction. The blockage close to the blade root was significantly reduced by slotting. However, the blockage ratio in an area greater than 25%H slightly increased for the prototype, which was caused by an increase in the flow near the blade root once the cascade flow was fixed. The blowing ability of the slotted channel for a low-energy fluid increases with height. The low-energy fluid was constrained to a smaller height range, and the flow capacity near the blade root was further increased.

Figure 18 shows the total pressure loss contours and streamlines at 10% blade height. Two radial vortex systems comprise most of the prototype cascade loss at 10%H. However, varying the heights of the slotted channels has varying effects on the loss structure, particularly in this section. Case-5.22 arrangement reduces the scale of the vortex structure outside the suction surface and moves the vortex core towards the trailing edge. The separation on the outer side of the suction surface varied as the height increased. The high-energy fluid flows out of the slot and then flows close to the blade surface, canceling with the vortex system structure generated by the separation of the angular region and appearing at the trailing edge as another small-scale vortex structure due to the convergence of the jet flow with the main flow.

3.2.2 The Analysis Results of Variable Angle of Attack

The operating conditions of helium compressors regularly fluctuate owing to numerous factors that require a compressor with excellent stability. This section aims to determine whether the slotted cascade performs well aerodynamically under different inflow conditions. Case-8.53 can obtain a specific improvement effect; simultaneously, the damage to the structural strength of the blade is relatively small. To ensure that the test was carried out smoothly, the prototype cascade and Case-8.53 aerodynamic performance and flow field variation were analysed with different angles of attack in this section.

The curve between the pressurising capability of the cascade and the total pressure loss as a function of the angle of attack can somewhat represent the performance of the cascade. The characteristic curve is shown in Fig.19. The working fluid diffusion capacity is represented by the static pressure ratio in the cascade, and its formula is

$$\pi = P / P_{in} \tag{5}$$

where P denotes the static pressure at the measurement point. It can be concluded that slotting can reduce the loss and increase the pressure ratio of the prototype cascade within a selected angle of attack, as shown in Fig.19. The pressurisation ability of the cascade improves with an increase in the angle of attack.

Three angles of attack i.e. -4°, 0° and 4° are selected for further analysis. From Fig. 20, it can be observed that, for all angles of attack, the main affected area of the slotted channel was below 25%H and did not change with the selected angles. The improvement below 25%H became more prominent when the angle of attack shifted from negative to positive; however, the loss in the middle of the blade increased. When i=4°, slotting had the best blowing effect on the boundary layer of the end wall, thereby improving the flow in the corner region.

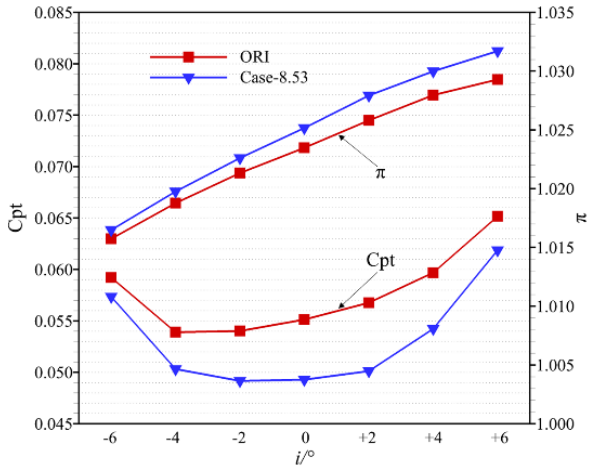

Fig. 19 Attack angle characteristic curves of two arrangements

Figure 21 shows the static pressure distribution and limit streamlines on the suction surface at different angles of attack. The blade root slotting mainly influenced the downstream flow field of the slotted channel outlet. Its effect is visible in changing the blade trailing-edge wall's separation structure, delaying the corner separation's generation points, and inhibiting the development of corner separation in the radial direction. The low-energy flow at the corner increases in velocity as part of the fluid flowing out of the channel moves in the flow direction. The other part is squeezed by the trailing edge reflux and advances towards the blade centre, forming a new separation line. Hence, the static pressure at the trailing edge of the blade increased significantly with an increase in attack angle. When a slot was added, the separation line structure at the end wall of the trailing edge became more regular. This demonstrates that the working-fluid flow in the cascade can be effectively organised with the addition of a slot.

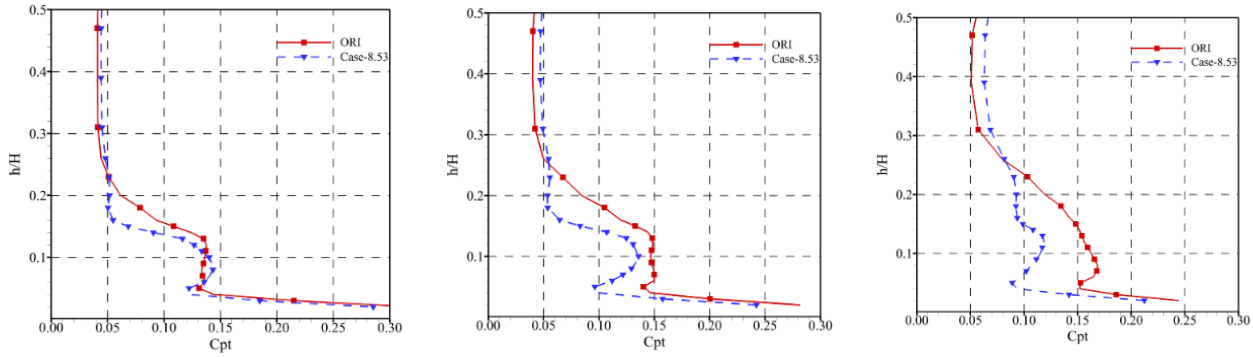

(a)i=-4° (b)i=0° (c)i=4°

Fig. 20 Outlet cross-section losses along the blade height for different angles of attack

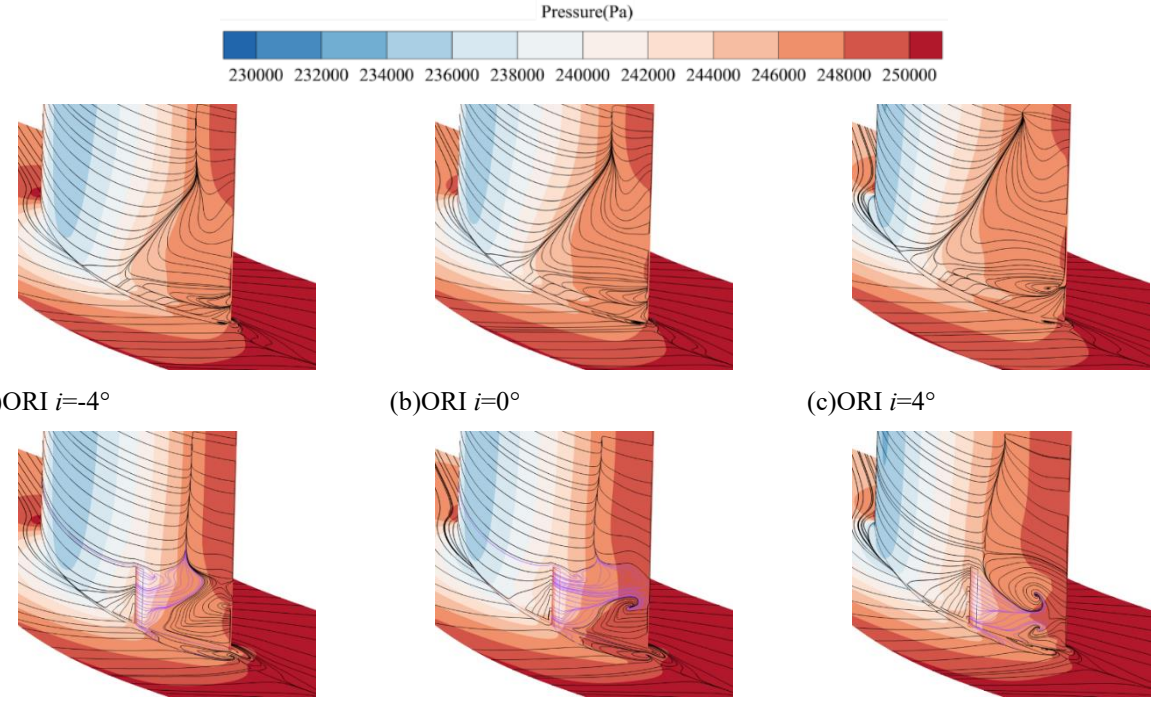

(a)ORI i=-4° (b)ORI i=0° (c)ORI i=4°

(d)Case-8.53 i=-4° (e)Case-8.53 i=0° (f)Case-8.53 i=4°

Fig. 21 Static pressure distribution and the limit streamline the suction surface for different angles of attack

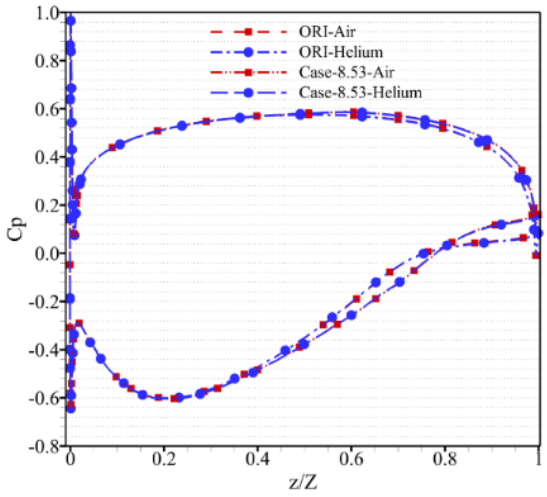

Fig. 22 Distribution of static pressure coefficient of different schemes with 20% blade height section under different working fluids

4. EXPERIMENTAL VERIFICATION OF NUMERICAL RESEARCH ON BLADE ROOT SLOTTING OF HELIUM COMPRESSOR

Helium is a unique working fluid that is difficult to compress, and experimental studies on helium are expensive and challenging. In recent years, most scholars researching helium compressors have used an air compressor design and conducted experiments for validation. This section compares the numerical simulation results for helium as the working fluid and air under different operating conditions to demonstrate the feasibility of the alternative testing of helium with air as the working fluid. Experiments with air as the working fluid in the prototype and slotted cascades were conducted to verify the effectiveness of slotting on a high-load helium compressor cascade.

Figure 22 shows that at similar Reynolds and Mach numbers, the pressure distributions on the blade surface of the high-load blade profile calculated by numerical computation with air and helium were consistent. Slotting can increase the blade profile load by approximately 40%-75% of the chord length. The fluid downstream of the 75% chord length increased the static pressure near the trailing edge owing to the energy loss from the pressure surface and separation from the suction surface, which reduced the profile load.

To conclude, cascade air can be used for the helium compressor. To validate the effectiveness of slotting, the prototype, and Case-8.53 cascade were analyzed in wind tunnel experiments at the design Mach number, i.e., 0.3 Ma in this paper. Figure 23 shows the total pressure loss contours at the outlet section under different slotting arrangements and attack angles. Figure 2 shows that slotting compresses the height of the spanwise loss region of the prototype cascade from 30%H to the blade root while reducing the spanwise coverage of the core loss. The optimisation effect of slotting is more prominent at a positive angle of attack. These experimental phenomena are consistent with the numerical simulation results.

Figure 24 compares the average total pressure loss coefficients at the outlet. Owing to the deviation between the calibration condition of the five-hole probe and the actual experimental conditions, the outlet loss was generally higher than that in the numerical simulation results. The graph in Fig.24 shows that slotting decreases the cascade loss at every angle of attack. The effect of blade root slotting became more significant with increased attack angle. Therefore, the cascade loss decreases by 16.469% at an attack angle of 4°.

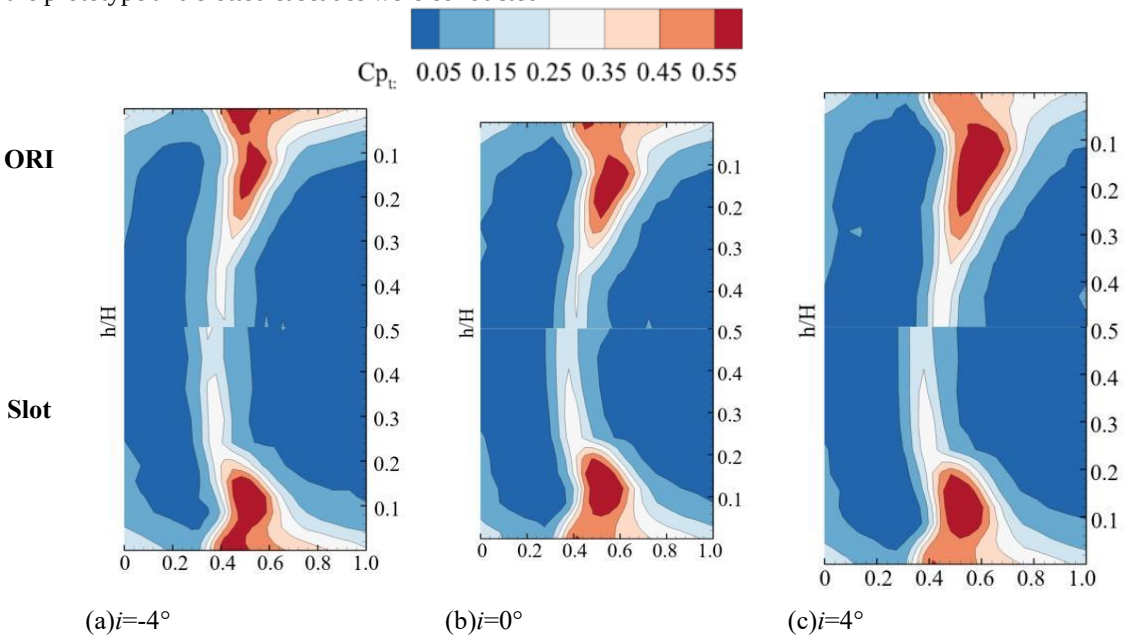

(a)*i*=-4° (b)*i*=0° (c)*i*=4°

Fig. 23 Total pressure loss distribution of measure plane

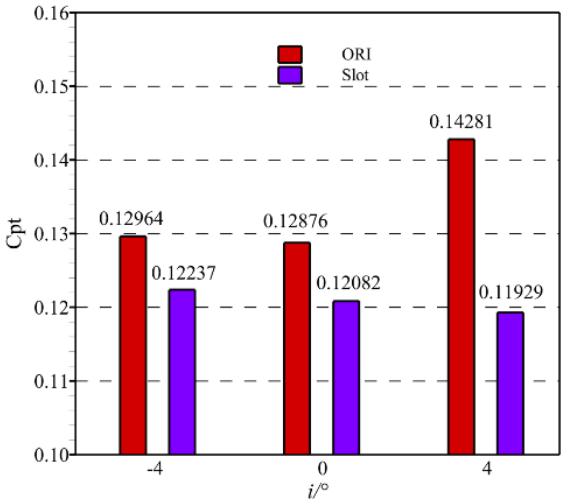

Fig. 24 Total pressure loss coefficient in measure plane for different angles of attack

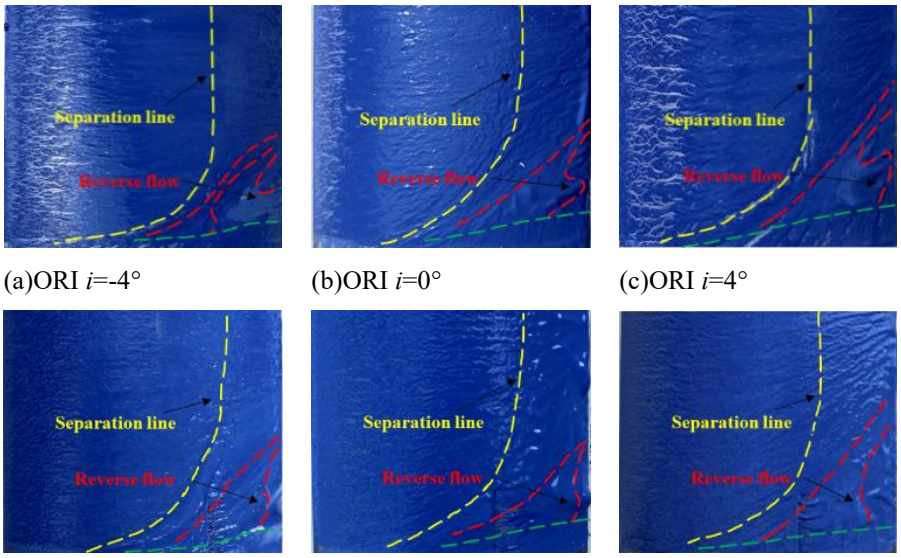

(a)ORI *i*=-4° (b)ORI *i*=0° (c)ORI *i*=4°

(d)Slot *i*=-4° (e)Slot *i*=0° (f)Slot *i*=4°

Fig. 25 Oil flow test of prototype cascade and slotted cascade

An oil flow test can be used to investigate the effects of blade root slotting on the limiting streamline on the suction surface under realistic cascade conditions. Simethicone, oleic acid, and blue pigment were mixed appropriately and allowed to settle for > 3 h to ensure proper viscosity and uniform color. Subsequently, the coating was uniformly applied to the suction surface of the blade, and the experiment was conducted. The limiting streamlines of flow at different attack angles are shown in Fig. 25. It can be observed that the streamline after slotting moves significantly backward compared to the prototype separation line with an increase in the attack angle, and the reverse flow region shortens radially and moves towards the blade root. The slotted blade utilize the pressure difference between the suction surface and the pressure surface to generate gap leakage flow, and the axial momentum of the leakage flow inhibits the over-turn of the lower end-wall surface layer boundary, thus reducing the negative impact of the layer boundary on the mainstream fluid.

5. CONCLUSIONS

In this study, a numerical simulation was performed to investigate the effects of the slotting profile and slotting height on the performance of a high-load helium compressor cascade, which fills the gap in the control technology of high-load helium compressor. In addition, the effect of varying the angle of attack was analysed. The numerical results were validated experimentally using air as the working fluid. The following conclusions were drawn:

1) The slot position was set at 65%*Ca* because the positioning of the slot at the upstream position was ineffective owing to the flow deviation from the blade profile and the smaller outlet angle. Accordingly, it is concluded that the total pressure loss coefficient is reduced when the slot entrance is positioned at the A2 point, and the slotted profile of Case 5 is used. This solution is more in line with the flow of the fluid

inside the channel and increases the axial momentum of the outlet fluid.

2) The axial momentum generated by the leakage vortices blows away the vortices formed due to the separation of corner area. The airflow flows close to the suction surface of the blade and breaks away at the trailing edge of the blade, merges with the main flow and forms a new vortex. As the height of the channel increases, the blowing away of the vortices in the corner region becomes more pronounced and the cascade improvement performance is better. The vortex core of the concentrated shedding vortex (CSV) flow towards the end wall, and the vorticity and influence area of the passage vortex (PV) and wall vortex (WV) are reduced.

3) Slotting reduced corner separation for all selected attack angles. The improvement in the cascade aerodynamic performance with the addition of slotting was prominent in the secondary flow loss and corner regions below 25%H. The separated flow intensity in the corner region was significantly reduced. Accordingly, the flow capacity of the high-load cascade increased because of the optimum positioning of the slotting close to the blade root.

4) The improvement effect of slotting on a high-load helium compressor was analysed experimentally. It was concluded that the total pressure loss coefficient of the slotted cascade was reduced by 6.167% compared with that of the prototype cascade at the design attack angle. Accordingly, the improvement effect of the slotted cascade was 16.469% better than the prototype cascade at an attack angle of 4 °.

ACKNOWLEDGEMENTS

The authors are grateful for the financial support from the National Natural Science Foundation of China (52206042), the Liaoning Province Natural Science Foundation (2022-BS-096) and the Fundamental Research Funds for the Central Universities(3132023118).

CONFLICT OF INTEREST

There is no conflict of interest to be declared in this work.

AUTHORS CONTRIBUTION

Conceptualisation: **Z. Tian**.; Methodology: **Y. Fan** and **Z. Tian**; Software: **Y. Fan**; Validation: **Y. Fan**, **A. Malik**, and **P. Ren**; Formal analysis: **Y. Fan** and **P. Ren**; Investigation: **J. Zheng**; Resources: **Z. Tian**; Data curation: **Y. Fan** and **P. Ren**; Writing —original draft preparation: **Y. Fan**; Writing —review and editing: **A. Malik** and **Z. Tian**; Visualisation: **Y. Fan** and **P. Ren**; Supervision: **Z. Tian**; Project administration: **Z. Tian**; Funding acquisition: **Z. Tian**

REFERENCES

Brent, J. A. (1972 March31). *Single-stage experimental evaluation of compressor blading with slots and vortex generators.* NTRS - NASA Technical Reports Server. https://ntrs.nasa.gov/citations/19720015141

Chen, Y., Zou, Z., & Fu, C. (2019). A study on the similarity method for helium compressors. *Aerospace Science and Technology*, *90*, 115-126. https://doi.org/10.1016/j.ast.2019.04.026

El-Genk, M. S., & Tournier, J. M. (2008). Noble gas binary mixtures for gas-cooled reactor power plants. *Nuclear Engineering & Design*, *238*(6), 1353-1372. https://doi.org/10.1016/j.nucengdes.2007.10.021

Kadak, A. C. (2016). The status of the US high-temperature gas reactors. *Engineering*, *2*(1), 119-123. https://doi.org/10.1016/J.ENG.2016.01.026

Ke, T., & Zheng, Q. (2010). *The highly loaded aerodynamic design and performance enhancement of a helium compressor.* Asme Turbo Expo: Power for Land, Sea, and Air, 7, 431-442. https://doi.org/10.1115/GT2010-23116

Ke, T., & Zheng, Q. (2011 January). *Design and aerodynamic analysis of a highly loaded helium compressor*. ASME 2011 Turbo Expo: Turbine Technical Conference and Exposition. http://doi.org/10.1115/GT2011-46044

Ke, T., & Zheng, Q. (2012). Highly loaded aerodynamic design and three dimensional performance enhancement of a HTGR helium compressor. *Nuclear Engineering and Design*, *249*, 256-267. https://doi.org/10.1016/j.nucengdes.2012.03.029

Li, W., Liu, M., & Ji, L.(2023). Study on the trajectory of tip leakage vortex and energy characteristics of mixed-ffow pump under cavitation conditions. *Ocean Engineering*, *267*(2023), 113225. https://doi.org/10.1016/j.oceaneng.2022.113225

Liu, Y., Sun, J., Tang, Y., & Lu, L. (2016). Effect of slot at blade root on compressor cascade performance under different aerodynamic parameters. *Applied Sciences*, *6*(12), 421-421. https://doi.org/10.3390/app6120421

Malik, A., & Zheng, Q. (2020). Effect of helium xenon as working fluid on the compressor of power conversion unit of closed Brayton cycle HTGR power plant. *International Journal of Hydrogen Energy*, *45*(16), 10119-10129. https://doi.org/10.1016/j.ijhydene.2020.01.220

Ramzi, M., Bois, G., & Abderrahmane, Z. (2011). Numerical study of passive control with slotted blading in highly loaded compressor cascade at low mach number. *International Journal of Fluid Machinery and Systems*, *4*(1), 97-103. https://doi.org/10.5293/IJFMS.2011.4.1.097

Tian, Z. (2019). *Research on the performance and design method of helium compressor*. Harbin Engineering University. http://doi.org/10.27060/d.cnki.ghbcu.2019.000192

Tian, Z., Jiang B., Malik, A., & Zheng, Q. (2019). Axial helium compressor for high-temperature gas-cooled

reactor: A review. *Annals of Nuclear Energy*, *130*, 54-68. https://doi.org/10.1016/j.anucene.2019.02.032

Tian, Z., Wang, C., & Zheng, Q. (2021). Investigation of the effects of different working fluids on compressor cascade performance. *Applied Sciences*, *11*(5), 1989. https://doi.org/10.3390/app11051989

Weisbrodt, I. A. (1996, Augest01). *Summary report on technical experiences from high-temperature helium turbomachinery testing in germany*. International Atomic Energy Agency, Vienna (AT). United States. http://www.osti.gov/etdeweb/biblio/411378

Ye, Q., Su, G., Huang, W., Yang, Y., & Zhang, D. (2022). Research on development strategy of China nuclear energy modernization. *Science & Technology Review*, *40*(24), 20-30. http://kjdb.org/EN/10.3981/j.issn.1000-7857.2022.24.003

Yoon, S., Ajay, R., Chaluvadi, V., Michelassi, V., & Mallina, R. (2019 November 5). *A passive flow control to mitigate the corner separation in an axial compressor by a slotted rotor blade*. Asme Turbo Expo: Power for Land, Sea, and Air. https://doi.org/10.1115/GT2019-90754

Zhao, W., Jiang, B., Duan, Y., & Zheng, Q. (2021). Effect of partial clearance on the stability of axial compressor at low operating conditions. *Journal of Harbin Engineering University*, *42*(04), 528-534. https://doi.org/10.11990/jheu.201910061

Zhao, W., Jiang, B., Duan, Y., & Zheng, Q. (2022). Stator stall and partial clearance control of compressor. *Journal of Aerospace Power*, 1-12. https://doi.org/10.13224/j.cnki.jasp.20220164